A NUMERICAL SIMULATION OF PARTICLE DEPOSITION IN TURBULENT BOUNDARY LAYERS

G. A. KALLIO[1] and M. W. REEKS[2]

[1]Department of Mechanical Engineering, Chico State University, CA, U.S.A.
[2]Berkeley Nuclear Laboratories, CEGB, Berkeley, Glos. GL13 9BP, England

Abstract—A Lagrangian random-walk approach to modeling particle deposition in turbulent duct flows is presented. The inhomogeneous boundary layer turbulence is simulated by a discrete eddy field, characterized by a random normal velocity (drawn from a Gaussian probability distribution) and a random time scale (drawn from an exponential probability distribution). A mean streamwise velocity profile is superposed upon the turbulence field using the law-of-the-wall relations. The turbulent r.m.s. velocity and time scale profiles are obtained from experimental data. The particle equations of motion include Stokes' drag and shear-induced (Saffman) lift. The equations are numerically solved for particle relaxation times (τ^+) ranging from 0.3 to 1000 and particle-fluid density ratios of 500–5000. Approximately 500–10,000 particle trajectories are computed for each case, simulating particle deposition in pipe flow with a sticky wall. Deposition velocity predictions compare favorably with measurements, showing that inertial impaction is dominant at lower values. A predicted decrease in deposition velocity occurs for large particle ($\tau^+ > 30$) due to reduction in particle fluctuating velocity. Shear-induced lift increases particle deposition rate, most significantly for $1 < \tau^+ < 10$. Particle concentration profiles reveal that smaller particles ($\tau^+ < 10$) tend to accumulate in the near-wall region due to the sudden damping of fluid turbulence. Predicted particle r.m.s. velocity profiles compare favorably with measurements, showing a decrease in magnitude with increasing inertia.

Key Words: particles, deposition, turbulence

1. INTRODUCTION

The problem of predicting the deposition rate of small solid particles or liquid droplets from a turbulent gas stream on to an adjacent surface is common to many engineering situations, such as air cleaning, fouling/erosion of turbine blades, plate-out in nuclear reactor coolant circuits, aerosol sampling and microchip fabrication. Particle deposition is also an important process in numerous environmental concerns, such as acidic air pollution, river channel topology, sand dune movement and inhalation of toxic dusts. Mechanisms responsible for deposition can include inertial impaction, gravitational settling, electrostatic forces, thermophoresis, Brownian diffusion and lift forces. For electrically neutral particles within the diameter range 1–50 μm, the predominant mechanism is inertial impaction, which is the primary concern in this study. Moreover, inertial deposition due to turbulent fluctuations is probably the least understood and has been the most difficult to model and predict.

When faced with the task of modeling turbulent particle deposition, or any multiphase flow, two general approaches are possible. One is the Lagrangian approach, usually known as a "trajectory model", where the instantaneous motions of individual particles are tracked by solving their equations of motion. The trajectories of many particles (typically thousands) are realized in order to form the average behavior of the particle–fluid system. The other approach is Eulerian, often called a "two-fluid" model, where the particles are treated as a continuous phase, in much the same way that a tracer gas would be regarded in a binary mixture. The motion of the particulate phase is mathematically described by mass, momentum and energy conservation, similar to a fluid.

The first major deposition models utilized the two-fluid approach, employing what is commonly referred to as the "diffusion/free-flight" concept (Friedlander & Johnstone 1957; Davies 1966). In this model, particles are transported by turbulent diffusion (assuming Fick's law is valid) from the bulk of the flow toward the surface to within one particle stop distance, characterized by a particle's relaxation time and wallward velocity. At this point, particles are assumed to deviate from the local turbulent fluid motion, arriving at the surface through free-flight by virtue of their inertia. Deposition is usually assumed to be entirely limited by this final transport through the near-wall region, implying that the deposition rate should only depend upon the particle relaxation time when

normalized to wall variables. In the original theory, gradient–transport equations were solved using measured turbulence quantities, assuming that particle and fluid (eddy) diffusivities were identical throughout the flow. The equations were applied to the flow from the turbulent core to one stop distance from the wall, where particle concentration was assumed to vanish. While this concept has certain physical merit, it offers no method for determining the particles' free-flight velocity. As a result, this quantity must be arbitrarily specified, leaving a loophole for empiricism. In order to match existing deposition data, unrealistically high velocities must be used, corresponding to fluid velocities inside the turbulent core (Friedlander & Johnstone 1957). If local fluid velocities at the stop distance are employed, deposition is generally underpredicted by 1–2 orders of magnitude (Davies 1966). Despite these underlying problems, this model contained many novel ideas that are still used today.

Subsequent modeling efforts usually retained the basic diffusion/free-flight idea, but attempted to improve agreement with experimental data by an assortment of modifications (Beal 1970; Sehmel 1970). These included: (i) varying the free-flight distance from the wall; (ii) modifying the free-flight velocity; (iii) allowing particle diffusivity to differ from eddy diffusivity; and (iv) changing the concentration boundary condition at the free-flight distance. All the alterations were generally performed in an *ad hoc*, arbitrary manner. Often, the end-products of these "improvements" were empirical, nonunified sets of equations for calculating deposition models under rather restrictive conditions.

Some modified diffusion/free-flight models are worth discussing in more detail. Liu & Ilori (1974) proposed a new expression for particle diffusivity, containing an additional term to account for enhanced deposition by inertia. The local fluid velocity was used as the particle free-flight velocity at the stop distance, and the particle concentration there was estimated by assuming that the concentration profile was identical to the streamwise velocity profile. This latter assumption only applies to molecular species and it adds a Reynolds number dependency to the wall-variable-normalized deposition rate, which has little experimental confirmation. The model yielded reasonable agreement with deposition rate measurements for intermediate relaxation times, but poor agreement at high values. This is primarily due to the particle diffusivity expression, which increases in an unbounded manner with relaxation time and does not reflect the difference between the particle and fluid r.m.s. velocity. These deficiencies suggest that particle inertia does not solely manifest itself as an increased diffusivity in the boundary layer.

Lagrangian-type trajectory models have been used to a much lesser extent than Eulerian models in the prediction of turbulent particle deposition. The reason is primarily due to their computational expense and the difficulty in specifying boundary layer turbulence in a Lagrangian framework. In general, they provide a more detailed and realistic model of deposition due to the fact that the instantaneous equations of motion are solved for each particle through a field of random fluid eddies. Hutchinson *et al.* (1971) were the first to incorporate a stochastic element into deposition theory, even though their model retained an Eulerian format. Particle dispersion within the turbulent core flow was modeled as a two-dimensional diffusion process, where the particle diffusivity was determined by a Lagrangian random-walk simulation. This simulation considered individual particle–eddy interactions in assumed homogeneous turbulence (constant velocity and eddy time scales). This core region model was used to calculate the fraction of particles approaching the pipe wall at some near-wall location. The fraction of these particles actually impacting the wall was determined by a separate calculation, in which particles were assumed to travel by inertial projection (free-flight) through a stagnant annular region adjacent to the wall. The edge of this region was chosen to be at $y^+ = 1.25$ in order to match experimental data (where y^+ is the normalized wall coordinate). This choice indicates that the homogeneous core model was inappropriately applied to the strongly inhomogeneous buffer region ($y^+ < 30$). This contradiction raises skepticism since the basic behavior of the deposition process is governed by the inhomogeneity of the turbulent boundary layer. Despite this inconsistency, the model contains useful ideas that overcome some of the limitations of earlier models.

Reeks & Skyrme (1976) presented a model that was aimed to explain the experimentally-confirmed decline, or "roll-off", in deposition rate with increasing relaxation time beyond a certain large value. Following the concept used by Hutchinson *et al.*, they calculated the fractional free-flight penetration of particles through the viscous sublayer ($y^+ < 5$) based upon a Gaussian

distribution of particle velocities normal to the wall. This distribution was determined by solving the particle equation of motion using spectral energy density data from turbulent pipe flow. The model was successful in predicting the decrease in deposition at large relaxation times, however, an acceptable fit with data required adjustment of two parameters. More importantly, it showed that particle inertia affects deposition through the behavior of both the particle r.m.s. velocity in the core and the free-flight projection through the near-wall region. A subsequent model was proposed to predict deposition for smaller particle relaxation times using a modified gradient–transport concept (Reeks 1982, 1983). The modification consisted of an additional convection term proportional to relaxation time and the gradient of particle r.m.s. velocity. Local equilibrium values were used for the particle r.m.s. velocity and particle diffusivity was equated to the fluid diffusivity. The additional convective deposition mechanism (termed "turbophoresis") was shown to increase the deposition rate beyond that predicted by Davies' local equilibrium model, thereby yielding better agreement with measurements. These results were important in indicating that Fick's law (i.e. gradient diffusion) does not provide a complete description of particle motion in the turbulent boundary layer due to its inhomogeneous character.

The existence of organized structures in the wall region, known as bursts, was the basis of the trajectory-based deposition model of Cleaver & Yates (1975). Their flow field consisted of spatially-intermittent regions of downsweeps, modeled as two-dimensional stagnation-point flows. Only particles entrained within this flow were able to impact the wall, governed by inertia and interception. Those particles not captured within the downsweep area were assumed to escape to the turbulent core via upsweep motions (ejections). The model was limited by the approximate nature of the particle trajectory solution and the *ad hoc* treatment of the axial flow influence on deposition. The agreement with experimental measurements was acceptable only when "adjusted" for the axial flow and was restricted to a narrow range of particle relaxation times. However, the model was useful in stressing the importance of the particle–fluid density ratio on deposition and confirming the relative independence of deposition rate upon relaxation time at large values (high inertia).

It is apparent that existing models have been generally unsuccessful in producing satisfactory agreement with measured deposition rates. The limited success that has been achieved has required significant empiricism. This failure is primarily due to our present lack of understanding regarding turbulent particle dispersion (diffusion) in inhomogeneous flows. This is evidenced in Eulerian modeling approaches, which, because of the closure problem, require "educated guesses" of the relationship between particle velocities, time scales and concentration. Unfortunately there exists very little physics at present to guide these models.

The purpose of the present work is not necessarily to promote a new tool for predicting particle deposition, but to provide a better understanding of the physical details of the deposition process. A Lagrangian approach is utilized to provide a two-dimensional, numerical simulation of particle motion within the entire turbulent boundary layer of a duct (pipe or channel) flow. The turbulent flow is simulated by a random velocity field of random time scales, through which many thousands of particle trajectories are solved from the equation of motion to yield an average deposition rate. Particle concentration profiles and r.ms. velocities are also predicted by the simulation. This numerical "experiment" has the advantage of including the actual physics of the particle–fluid interactions without the *ad hoc* assumptions necessarily contained in the Eulerian-based diffusion models.

2. PARTICLE EQUATION OF MOTION

The general equation of motion for a small, rigid sphere in an unbounded flow contains many terms which can be justifiably neglected in most incompressible gas–particle systems since particle density is much greater than fluid density (Maxey & Riley 1983). These neglected terms include the pressure gradient force, virtual mass, Basset history integral and Faxen's modification to Stokes' drag force. The effects of gravitational settling (i.e. very large particles, $a \gtrsim 50 \, \mu m$) and Brownian diffusion (i.e. very small particles, $a \lesssim 0.3 \, \mu m$) are also not considered here. The unbounded equation of motion then reduces to a balance of Stokes' drag force, particle inertia and any body force that may be present:

$$m_p \frac{dV}{dt} = 6\pi\mu a (U - V) + F_{body},$$ [1]

where m_p is the particle's mass, $(4/3)\pi a^3 \rho_p$, t is time, a is the particle radius, ρ_p is the particle mass density, μ is the dynamic viscosity, U is the local fluid velocity, V is the particle velocity and $\mathbf{F}_{body}$ represents a body force on the particle. However, the turbulent boundary layer is a bounded flow, where the effects of the wall must also be accounted for. Such effects include an increase in drag coefficient (Happel & Brenner 1965; Davis 1972; Dahneke 1974), the lift force due to the imposed mean shear (Saffman lift) and the possible lift due to particle rotation (Magnus effect). Rizk & Elghobashi (1985) have shown that particle motion in turbulent flow near a plane wall is primarily affected by shear-induced lift, while the effect of the drag increase is comparatively small and confined to regions much closer to the wall. The additional lift caused by free rotation (i.e. no imposed spin) can be shown to be at least an order of magnitude less than shear lift. Thus, only the lateral lift on a freely-rotating sphere in a uniform simple shear flow is considered here, given by Saffman (1965, 1968) as

$$F_L = 6.46\,\mu a^2 \sqrt{\frac{\kappa}{v}}\,V_r, \qquad [2]$$

where κ is the local fluid velocity gradient, v is the kinematic viscosity and V_r is the particle velocity relative to that of the fluid along the center streamline. This derivation is restricted to low Reynolds numbers, representing relatively large shear ($\kappa v/V_r^2 \gg 1$) and small particle sizes ($\kappa a^2/v \ll 1$). In addition, [2] is strictly valid for uniform shear (linear velocity gradient), however, the departure from linearity in the turbulent boundary layer is negligibly small outside the viscous sublayer over the characteristic length scale associated with the lift, $\sqrt{v/\kappa}$.

It is evident that particle motion in at least two dimensions, streamwise (x) and normally (y), must be considered to simulate deposition in the boundary layer. Figure 1 defines this coordinate system. Velocity variation in the spanwise (z) direction is assumed negligible. Excluding body forces, the equations of motion can now be expressed as

$$m_p \frac{dv_x}{dt} = 6\pi\mu a(u_x - v_x), \qquad [3]$$

and

$$m_p \frac{dv_y}{dt} = 6\pi\mu a(u_y - v_y) + 6.46\,\mu a^2 \sqrt{\frac{1}{v}\frac{du_x}{dy}}\,(u_x - v_x). \qquad [4]$$

Due to the self-similarity of the turbulent boundary layer, it is convenient to normalize these equations with respect to the wall variables, kinematic viscosity (v) and friction velocity (u_*), yielding

$$\frac{dv_x^+}{dt^+} = \frac{u_x^+ - v_x^+}{\tau^+} \qquad [5]$$

and

$$\frac{dv_y^+}{dt^+} = \frac{u_y^+ - v_y^+}{\tau^+} + 0.727 \sqrt{\frac{\dfrac{du_x^+}{dy^+}}{\left(\dfrac{\rho_p}{\rho_f}\right)\tau^+}}\,(u_x^+ - v_x^+), \qquad [6]$$

where $y^+ = tu_*^2 v$, $u^+ = u/u_*$, $v^+ = v/u_*$ and

$$\tau^+ = \frac{2\left(\dfrac{\rho_p}{\rho_f}\right)a^2 u_*^2}{9v^2}. \qquad [7]$$

It can be seen from [5] and [6] that a particle's trajectory through the boundary layer is governed by two dimensionless parameters in addition to the fluid velocity field. These parameters are the normalized particle relaxation time (τ^+), and the particle–fluid mass density ratio (ρ_p/ρ_f). This relaxation time, or Stokes number, is a measure of a particle's inertia relative to the viscous drag that it experiences. It is related to the particle stop distance $s^+ = v^+\tau^+$, which indicates the degree to which a particle trajectory may deviate from fluid streamlines. Note that for a fixed relaxation time, the particle–fluid density ratio also specifies the normalized particle radius, $a^+ = au_*/v$.
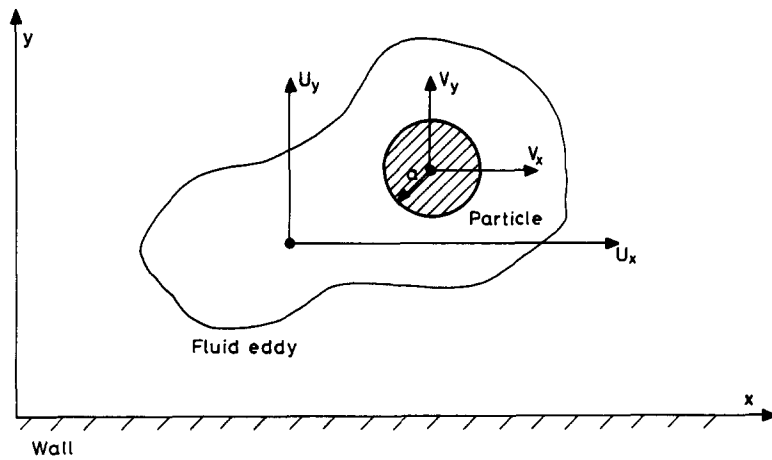
Figure 1. Coordinate system for solving two-dimensional particle equations of motion.

The nature of the lift force is interesting. If a particle leads to the fluid motion $(v_x > u_x)$, then the lift force is negative and the particle moves "down" the velocity gradient towards the wall. Conversely, if the particle lags the fluid $(v_x < u_x)$, then the lift is positive and it moves "up" the velocity gradient away from the wall. Hence, the lift force imposes no net drift on the particles; it only causes a particle to move faster and further in its original normal direction than it would in the absence of shear. This leads to an increase in particle r.m.s. velocity in the turbulent boundary layer, as predicted by Rizk & Elghobashi (1985). Also, [6] shows that the lift force will be most prominent for large τ^+ and small ρ_p/ρ_f.

3. TURBULENT FLOW FIELD

Ideally, one needs to know the entire Lagrangian time history of the turbulent boundary layer flow in order to precisely track the motion of discrete particles using [5] and [6]. Since such information is not practical to predict or measure, approximations must be employed to specify the flow field. In this study, the turbulent flow is simulated by a two-dimensional, random velocity field where the mean and r.m.s. profiles are specified according to established experimental results. The fluid flow is assumed to be unaffected by the momentum of the particle phase, thus representing a dilute suspension.

The mean streamwise velocity component is defined by the well-known law-of-the-wall relations for the viscous sublayer and logarithmic region (Hinze 1975, pp. 626–628):

$$u_x^+ = y^+ \qquad \text{for } y^+ \leqslant 5 \tag{8}$$

and

$$u_x^+ = 2.5 \ln y^+ + 5.5 \qquad \text{for } y^+ \geqslant 30. \tag{9}$$

The buffer region velocity distribution is obtained from a cubic spline interpolation, insuring that the velocity gradient used in the lift force term is continuous throughout the boundary layer:

$$u_x^+ = a_0 + a_1 y^+ + a_2 y^{+2} + a_3 y^{+3} \qquad \text{for } 5 < y^+ < 30, \tag{10}$$

where $a_0 = -1.076$, $a_1 = 1.445$, $a_2 = 0.04885$ and $a_3 = 0.0005813$. Streamwise turbulence is neglected in this simulation due to the dominant mean velocity and so would have little effect on particle deposition on to a smooth plane wall.

The normal velocity component consists solely of a fluctuating term whose r.m.s. spatial distribution is obtained by curvefitting the combined experimental data of Laufer (1954), Bremhorst & Walker (1973) and Kreplin & Eckelmann (1979). Unfortunately, r.m.s. velocity data very near the wall $(y^+ < 5)$ is limited and displays much scatter due to measurement difficulty (probe–wall interference effects). However, the electrochemical wall probe measurements of Finnicum &

Hanratty (1985) and the near-wall modeling work of Chapman & Kuhn (1986) indicate that the wall turbulence limit is quadratic in y^+, given by $u_y' \simeq 0.005y^{+2}$. Incorporating this limit into the curvefit function, the following fit to the normal r.m.s. velocity data is obtained, valid for $0 < y^+ < 200$:

$$u_y' = \frac{0.0005y^{+2}}{1 + Cy^{+n}},$$ [11]

where $C = 0.002923$ and $n = 2.128$.

A particle's trajectory through the boundary layer is modeled as a succession of interactions with turbulent eddies. Each eddy is characterized by a discrete random normal velocity and a discrete random time scale. This random-walk, or Monte-Carlo, approach has been used successfully in previous studies of particle dispersion in turbulent jets and grid-generated turbulence (Yuu et al. 1978; Shuen et al. 1983; Chen & Crowe 1983). The particle–eddy interaction time is assumed to be identical to the eddy time scale (or lifetime), even though inertia may cause a particle to traverse an eddy before it decays. However, the analysis by Reeks (1977) and the measurements by Wells & Stock (1983) show that inertia has only a minor effect on the long-time particle diffusivity in typical homogeneous turbulence. This situation arises because the inertia-reduced particle velocity fluctuations are nearly compensated by an increase in the integral time scale. Therefore, this shortened interaction time is not considered in this simulation. It should be noted, though, that such considerations are important when strong body forces are present, leading to the "crossing trajectories" effect (Csanady 1963).

The instantaneous eddy velocity (u_y^+) that a particle encounters along its path is determined by randomizing the r.m.s. normal velocity given by [11],

$$u_y^+ = u_y'^+ N_r,$$ [12]

where N_r is a random number drawn from a Gaussian probability density distribution of zero mean and unity standard deviation. The appropriate eddy time scale is assumed to be the Lagrangian integral time scale (T_L), representing the larger scale, more energetic, turbulent motions. The instantaneous time scale is specified by randomizing the integral scale from an exponential probability density distribution. An exponential distribution is used since it closely approximates the Lagrangian time correlation behavior. The necessity of randomizing T_L has been found in separate "test cases" involving the simulation of point-source particle dispersion in homogeneous turbulence. This feature insures that the simulated turbulence is stationary and yields self-consistent dispersion properties, i.e.

$$\overline{u'^2} T_L = \frac{1}{2} \frac{d\overline{Y}^2}{dt},$$ [13]

where $\overline{Y}^2$ is the mean-square displacement of the particle cloud. If the eddy time scale is fixed, the simulated turbulence is no longer stationary and [13] is not satisfied. The actual particle diffusivity will be in error (too small) by a factor of one-half.

The Lagrangian integral time scale is difficult to measure and so is usually estimated from Eulerian statistics. In homogeneous and isotropic turbulence, there exists experimental evidence to show that the Lagrangian and Eulerian integral scales are proportional, $T_L = \beta T_E$, where the Eulerian scale (T_E) is measured in the frame relative to which the mean velocity is zero. The "constant" β is generally regarded to be approx. 0.4 (Hinze 1975, p. 426). However, recent measurements by Sato & Yamamoto (1987) show that β is a function of the turbulent Reynolds number $(Re_\lambda = u'\lambda/\nu)$, varying from 0.6 to 0.3 for $Re_\lambda = 20$ to 70. Thermal diffusion measurements in grid-generated turbulence by Ferguson (1986) also corroborate these findings, yielding $\beta \simeq 0.34$ for $Re_\lambda = 50$ to 60. Similar measurements in inhomogeneous turbulence are not presently available, however, turbulence kinetic energy (k) and dissipation rate (ϵ) measurements in the boundary layer (Laufer 1954) can be used to estimate β and the integral time scale. Using $\lambda_G^+ = \sqrt{10k^+/\epsilon^+}$ for the normalized Taylor microscale (Hinze 1975, p. 219), Laufer's pipe flow data show that Re_λ ranges between 20 and 60 for $5 < y^+ < 200$. Therefore, the variation in β within the boundary layer can be reasonably estimated according to Sato & Yamamoto's results. Furthermore, T_E is proportional
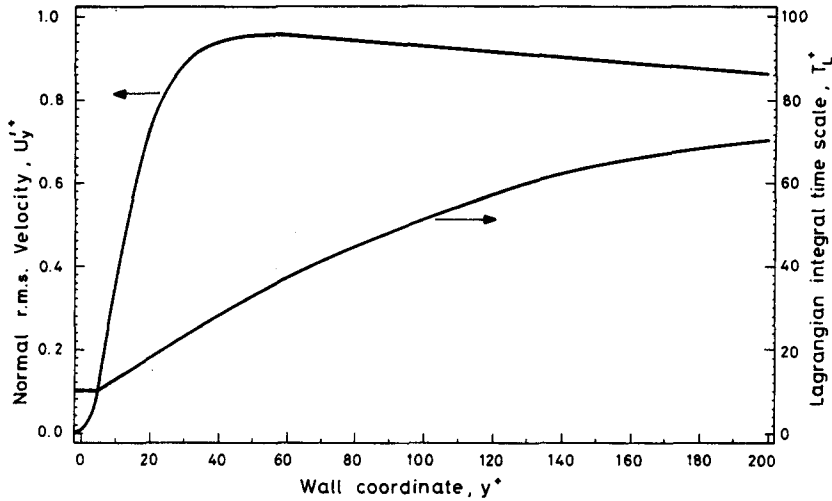
Figure 2. Normal r.m.s. fluid velocity and Lagrangian integral time scale distributions within the turbulent boundary layer.

to k/ϵ, where both Sato & Yamamoto's and Ferguson's data show this proportionality constant to be about 0.8. Therefore, the Lagrangian integral time scale can be estimated by

$$T_L^+ \simeq 0.8\beta(\text{Re}_\lambda)\frac{k^+(y^+)}{\epsilon^+(y^+)}. \qquad [14]$$

The time scale distribution over the boundary layer is obtained by curvefitting a polynomial to [14] using Laufer's kinetic energy and dissipation data, valid for $5 \lesssim y^+ < 200$:

$$T_L^+ = b_0 + b_1 y^+ + b_2 y^{+2}. \qquad [15]$$

where $b_0 = 7.122$, $b_1 = 0.5731$ and $b_2 = -0.001290$. Dissipation rate data within the viscous sublayer are very limited, but measurements of organized near-wall structures (bursting events) have indicated that the time scale is approximately constant at $T_L^+ \simeq 10$ in the near-wall region (Wallace et al. 1972; Brodkey et al. 1974; Luchik & Tiederman 1987). The simulation employs this constant time scale from the wall to $y^+ = 5$ and [15] is used for the remaining boundary layer region. Figure 2 shows the time scale variation within the boundary layer from [15] and the normal r.m.s. velocity curvefit from [14].

4. SIMULATION METHOD IN DUCT FLOW

The turbulent deposition rate to the duct wall is determined in a way similar to which one would measure it in a laboratory, hence, this approach is often called a "numerical experiment". Particles are "released" into the boundary layer from 20 equispaced locations over the range $0 < y^+ < 200$, thereby approximating a uniform injection. The streamwise initial velocity is set equal to the local (mean) fluid velocity while the normal initial velocity is randomized about the local equilibrium value (Reeks 1977):

$$u_{x0}^+ = u_x^+ \qquad [16]$$

and

$$v_{y0}^+ = \frac{u_y'^+ N_r}{\sqrt{1 + \dfrac{\tau^+}{T_L^+}}}. \qquad [17]$$

Each particle is tracked through the duct as it interacts with the simulated turbulence described in section 3. The instantaneous fluid eddy velocity, as prescribed by [12], is randomly drawn at the beginning of a particle–eddy interaction. The r.m.s. velocity value corresponds to the particle initial position and is allowed to vary throughout the interaction acording to [11]. The random component

is constant during the interaction. The eddy time scale, or interaction time, is randomly drawn from an exponential probability distribution with a mean prescribed by [15]. Its value corresponds to the particle's initial position and is held constant until that time has expired. A new eddy is then encountered and the process is repeated with a new initial position.

The differential equations of motion describing each particle–eddy interaction are solved numerically by a stiff system integrator utilizing the backward differentiation technique. The equations are repeatedly solved for each eddy encountered until the particle reaches a desired downstream position or collides with the duct wall. A zero-particle flux (symmetry) condition is imposed at $y^+ = 200$, representing a vanishing particle concentration gradient due to the nearly homogeneous turbulence. This condition is enforced in the simulation by replacing each particle that traverses this boundary with one of opposite velocity. During a particle's trajectory through the duct, its position and velocity are recorded at five streamwise stations, typically located at $x^+ = 2000, 5000, 10,000, 20,000$ and $50,000$. Each station consists of 20 equal collection intervals, or "bins", across the boundary layer, at which the location and velocity of each passing particle is recorded. Thus, particle concentration, mean velocity and r.m.s. velocity profiles can be calculated and their development along the duct can be observed.

Upon particle–wall impact, the streamwise position is recorded and the particle is assumed to be permanently removed from the flow, i.e a "sticky wall" condition is imposed so no rebounding or resuspension is considered. The fate of several thousand particles (typically 5000) over a given duct length determines the particle deposition rate, or deposition velocity. The deposition velocity (K) is defined as a mass transfer coefficient, relating the particle flux at the wall (j_w) to the average particle concentration in the boundary layer ($\bar{c}$), $j_w = K\bar{c}$. By relating the streamwise gradient in $\bar{c}$ to the wall flux and integrating over a length of duct, an expression for calculating K^+ (normalized to the friction velocity) can be obtained:

$$K^+ = \frac{\bar{U}A}{u_* P \Delta x} \ln\left(\frac{N_{in}}{N_{out}}\right), \qquad [18]$$

where $\bar{U}$ is the average streamwise fluid velocity across the boundary layer, A is the boundary layer cross-sectional area, P is the duct perimeter, Δx is the incremental length of duct considered, and N_{in} and N_{out} are the total number of particles entering and exiting the boundary layer, respectively. The total duct length is typically divided into 25 equal segments and the deposition velocity is computed per segment. This allows determination of the equilibrium deposition rate. This procedure closely conforms to the method by which deposition velocity is measured in most experimental investigations.

It should be noted that a true equilibrium in particle concentration does not occur in this problem since the total number of particles is continually being depleted along the duct. However, a quasi-equilibrium is achieved when the normalized concentration, i.e. $c(y)/\bar{c}$, no longer varies in the streamwise direction. The development of this steady-state concentration profile corresponds to a unique deposition velocity. As mentioned before, such equilibrium is assured in the simulation by monitoring the particle concentration profile and deposition velocity as a function of streamwise location until steady values are attained.

5. RESULTS

Three types of information were of primary interest in this computer simulation of particle deposition: (i) deposition velocity as a function of τ^+ and ρ_p/ρ_f; (ii) particle concentration profiles as a function of τ^+; and (iii) r.m.s. velocity profiles as a function of τ^+.

Deposition velocity computations are compared with the experimental measurements of Liu & Agarwal (1974) in figure 3 as a function of particle relaxation time. These measurements represent the deposition of olive oil droplets from a turbulent air stream inside a smooth glass tube, thereby insuring perfect sticking. Very good agreement exists for the entire range of relaxation times, including the roll-off in K^+ beyond about $\tau^+ = 30$. This characteristic is directly attributable to the reduced r.m.s. velocities of very massive particles, leading to a decrease in their deposition rate. Similar results are also predicted by Reeks & Skyrme (1976) using a diffusion/free-flight model. This agreement between experimental data and two models of entirely different methodology clearly

refutes the hypothesis that such roll-off is due to particle rebound or reentrainment (Papavergos & Hedley 1984).

Figure 3 also shows how deposition is affected by the inclusion of Saffman's lift force in the particle equations of motion. It is clear that lift increases the deposition velocity for all relaxation times, being most prominent between $\tau^+ = 1$ and $\tau^+ = 10$. As reported by Rizk & Elghobashi (1985), the primary effect of lift is to increase the particle normal r.m.s. velocity in the strong shear region near the wall. This increased r.m.s. velocity can be viewed as producing a higher particle diffusivity, thus enhancing particle deposition as would increasing the fluid turbulence.

It should be reiterated that Saffman's expression for shear-induced lift is somewhat restrictive for calculations within the turbulent boundary layer. The condition $\kappa a/v \ll 1$, when applied to the viscous sublayer ($\kappa = 1$), translates to $a^{+2} \ll 1$ in normalized form. This corresponds to $\tau^+ \ll 200$ for the Liu & Agarwal conditions, which invalidates the use of this expression for very massive particles. The shear restriction, $\kappa v/V_f \gg 1$, translates to $(\mathrm{d}u_x^+/\mathrm{d}y^+)/|u_x^+ - v_x^+| \gg 1$, which was monitored during the simulations and found to be frequently violated when $\tau^+ \gtrsim 10$ and $y^+ \gtrsim 30$. In addition, [2] was derived for uniform shear of infinite extent and so it is not strictly applicable to the wall region. Furthermore, there is experimental evidence that the near-wall particle lift is significantly higher than Saffman's value (Hall, 1988). In view of these restrictions, the effect of lift displayed in figure 3 should be regarded as approximate.

The particle–fluid mass density ratio affects particle deposition in two different ways. Firstly, [6] shows that an increasing density ratio will tend to reduce the effect of lift and so will lower the particle r.m.s. velocity and deposition rate. Secondly, for a given relaxation time, the density ratio is inversely related to particle radius (a^+); thus, deposition by the mechanism of interception will be significantly affected by ρ_p/ρ_f. This is shown in figure 4. Note that interception effects become quite prominent when particle inertia is removed, i.e. for small relaxation times. In fact, particle deposition is essentially governed by interception alone for $\tau^+ < 1$ until Brownian diffusion becomes important.

Equilibrium particle concentration profiles across the boundary layer are shown in figure 5 for small and large relaxation times. Note that the reduction in deposition with decreasing τ^+ is accompanied by a significant build-up in concentration near the duct wall. While these results do not include lift, similar profiles were computed when lift was included. It appears that this interesting feature is solely due to the nature of the turbulence in the boundary layer. The large gradient in normal fluctuating velocity in the buffer region ($5 < y^+ < 30$) forms an effective "trap" for particles with too little inertia to be projected across the relatively quiescent viscous sublayer. Such behavior was also mentioned by Hutchinson et al. (1971) but not explicitly presented. Very similar concentration profiles have been predicted by Reeks (1982) using a modified diffusion/free-flight model. This model includes a wallward drift velocity (turbophoresis) in the particle transport
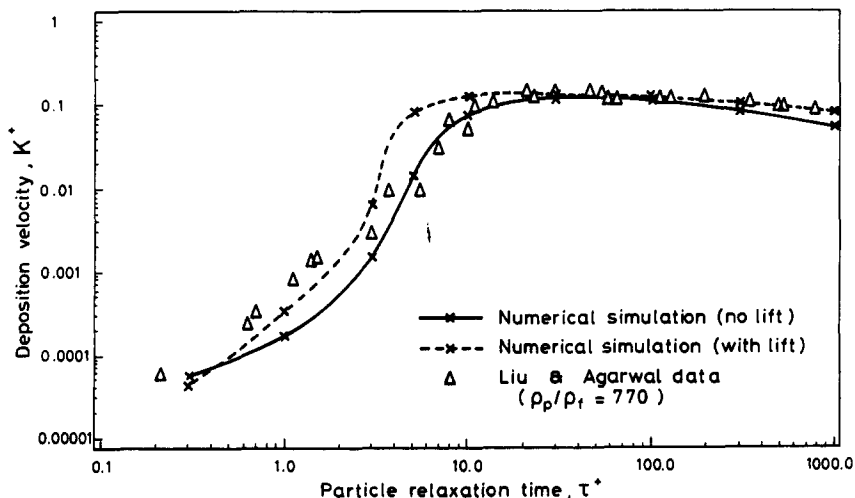

Figure 3. Comparison of numerical predictions with Liu & Agarwal's (1974) experimental deposition velocity data as a function of particle relaxation time.
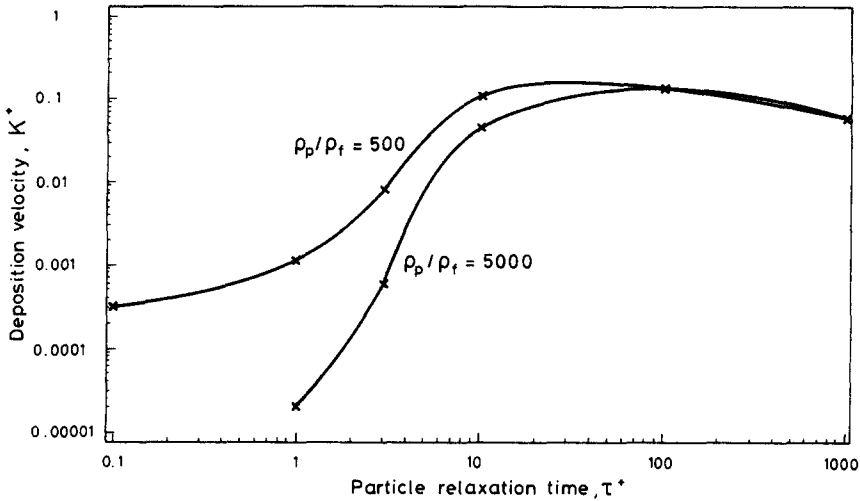
Figure 4. Effect of interception mechanism on deposition velocity predictions.

equation, arising from the normal gradients in boundary layer turbulence. This drift term is shown to attain a maximum value at $y^+ \sim 10$ for $\tau^+ \lesssim 1$ and so is primarily responsible for the build-up in particle concentration at $y^+ \sim 1$. The prediction of these near-wall peaks in concentration by two different and independent methods indicates that this phenomenon is real. Unfortunately, no detailed measurements of particle concentration within the viscous sublayer have yet been made. Concentration build-up in pipe flow has been reported to occur near the wall, however, this effect was only evident for larger particles and so was probably due to reentrainment (Sehmel 1970).

Finally, particle r.m.s. velocity profiles for various relaxation times are compared with the recent velocity measurements of Goren & Erhart (1989) in figures 6(a–c). These measurements were made by laser Doppler anemometry using oleic acid droplets in turbulent pipe flow. Several particle sizes and flow conditions were employed, producing normalized relaxation times ranging from $\tau^+ = 0.067$ to 14.3. Velocity measurements were limited to $y^+ > 12$ due to LDA signal degradation by light scattering from the wall. Good agreement between the simulation results and data is evident, showing that particle r.m.s. velocity differs significantly from that of the fluid down to $\tau^+ \sim 1$. The slight raggedness of some of the computational profiles can be attributed to velocity averages based upon an insufficient number of "collected" particles. Obviously, by increasing the number of particle realizations, a smoother curve could be obtained. Also shown for comparison is the r.m.s. velocity
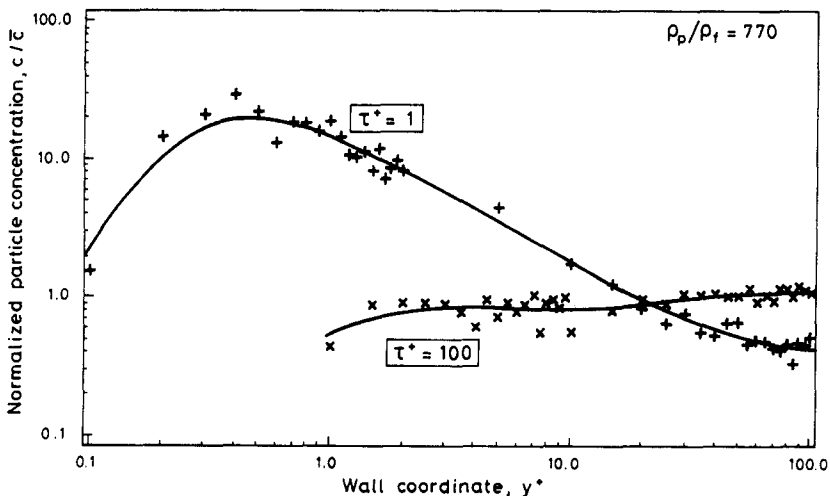

Figure 5. Predicted particle concentration profiles within wall region for $\tau^+ = 1$ and $\tau^+ = 100$ (solid line represents a best-fit curve to numerical results).
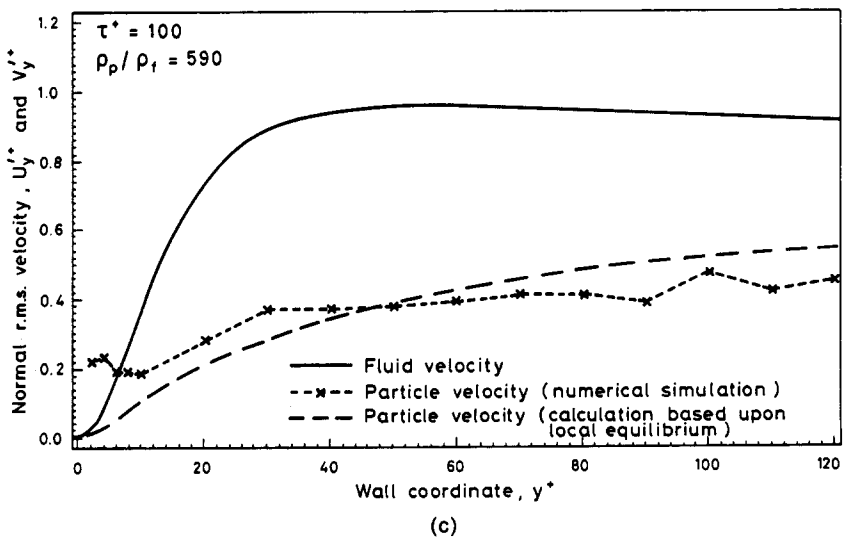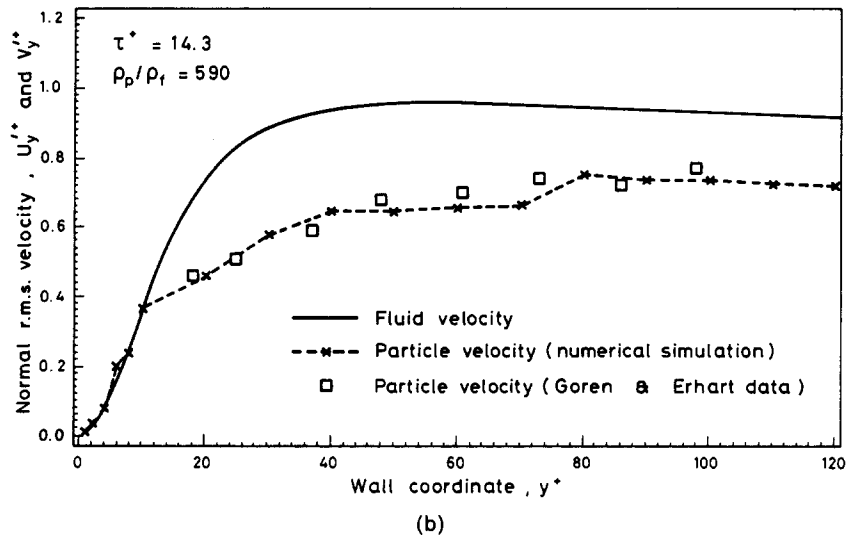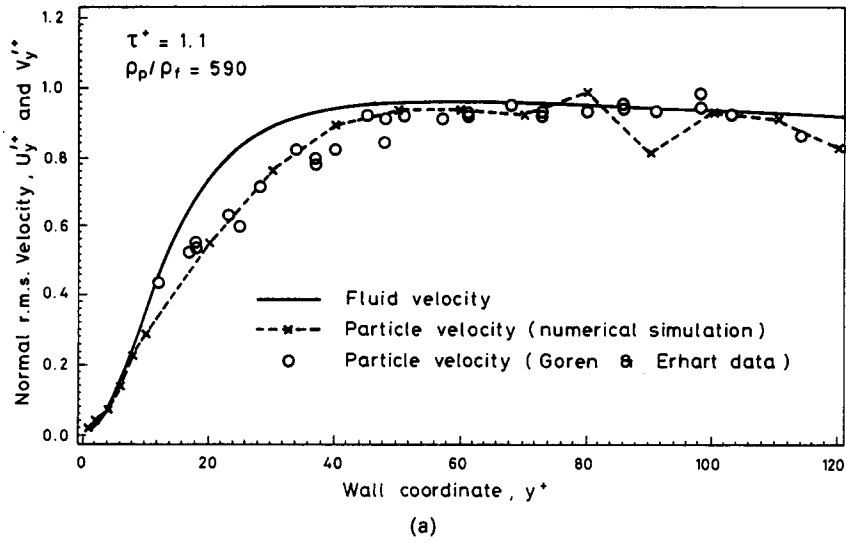
Figure 6. Comparison of predicted particle r.m.s. velocities with Goren & Erhart's (1989) experimental data within the turbulent boundary layer: (a) $\tau^+ = 1.1$; (b) $\tau^+ = 14.3$; (c) $\tau^+ = 100$.

profile computed under the assumption that particles come to equilibrium with the local fluid turbulence using [17]. This discrepancy clearly shows that equilibrium theory cannot, in general, be used to predict particle motion in the inhomogeneous turbulent boundary layer.

The use of Stokes' drag law in the numerical simulation is a reasonable approximation for comparison with the quoted experimental measurements. The largest droplets and highest flow rates employed in Liu & Agarwal's (1974) experiment yield a particle Reynolds number of about 4. This corresponds to a maximum error in predicted droplet velocity of approx. 7%, applying a typical correction term to Stokes' drag.

6. CONCLUSION

The described Lagrangian-based, stochastic model provides a detailed and realistic simulation of particle deposition in turbulent duct flows. Good agreement with experimentally-measured deposition velocities has been shown over the particle relxation time range of $\tau^+ = 0.3$ to 1000. Prediction of deposition rates at lower values of τ^+ will require the addition of Brownian diffusion effects. Of significance is the predicted decrease in deposition velocity for large particles ($\tau^+ \gtrsim 30$), corresponding to the reduction in particle r.m.s. velocity with increased inertia. This trend has been erroneously associated with particle wall bounce or reentrainment in earlier discussions. Particle interception is shown to be a dominant deposition mechanism for $\tau^+ < 10$, which may help explain the scatter of experimental data for particles of varied mass density. The effect of shear-induced lift on deposition rate appear to be significant for $1 < \tau^+ < 10$, slightly increasing the deposition velocity within this range. However, the applicability of Saffman's lift expression to the near-wall region is presently uncertain, so these results can not be viewed as exact.

Predicted particle r.m.s. velocities also compare favorably with LDA velocity measurements taken inside the boundary layer. These results clearly show that particle velocities are typically lower than the fluid r.m.s. velocity outside the wall region ($y^+ \gtrsim 30$), but can be greater than the local fluid velocity near the wall due to their inertia and the sudden damping in turbulence. This large gradient in fluid r.m.s. velocity in the buffer region also affects the particle concentration profile, allowing small particles ($\tau^+ < 10$) to accumulate in the relatively "laminar" wall layer. As a result, steady-state peaks in concentration are predicted that exceed the core concentrations by more than an order of magnitude. This interesting result has been reported in other theoretical studies, but genuinely needs some experimental confirmation.

It is evident from these results, namely the predicted concentration and r.m.s. velocity profiles, that particles in the boundary layer do not attain local equilibrium with the surrounding fluid turublence. This situation arises from the strong inhomogeneity (gradient) in fluid r.m.s. velocity within the buffer region. Thus, inertia allows a particle to retain some memory of the vigorous turbulent fluctuations from the homogeneous core as it travels into the suddenly quiescent wall region. This nonequilibrium situation precludes the use of simple gradient-diffusion ideas (i.e. Fick's law) since these are based upon local equilibrium theory. Therefore, some recognition of the inhomogeneity of boundary layer turbulence must be made in Eulerian-type particle flow models (e.g. diffusion/free-flight models) in order to properly describe the deposition process.

A vast amount of information can be extracted from this simulation due to its discrete and instantaneous treatment of particle motion. While not included in this paper, particle–wall impacts (speed and angle) statistics are readily predicted. Also, impact adhesion characteristics can be included to predict rebound and its effect on particle concentration near the wall. Furthermore, other deposition mechanisms such as gravitational settling, thermophoresis and electrostatic forces can be easily incorporated.

The major drawbacks in using this trajectory approach are the difficulty in simulating the Lagrangian-frame turbulence characteristics and the relatively high computational expense. The latter disadvantage will no doubt be partially alleviated as larger and more efficient computers are built. However, a two-fluid approach will generally yield the most cost-effective results, and for this reason, improvements in Eulerian modeling should be pursued. In this context, the understanding gained from such simulations may provide new modeling concepts in predicting particle deposition from time-average conservation equations.

REFERENCES

BEAL, S. K. 1970 Deposition of particles in turbulent flow on channel or pipe walls. *Nucl. Sci. Engng* **40**, 1–11.

BREMHORST, K. & WALKER, T. B. 1973 Spectral measurements of turbulent momentum transfer in fully developed pipe flow. *J. Fluid Mech.* **61**, 173–186.

BRODKEY, R. S., WALLACE, J. M. & ECKELMANN, H. 1974 Some properties of truncated turbulence signals in bounded shear flows. *J. Fluid Mech.* **63**, 209–224.

CHAPMAN, D. R. & KUHN, G. D. 1986 The limiting behaviour of turbulence near a wall. *J. Fluid Mech.* **170**, 265–292.

CHEN, P. P. & CROWE, C. T. 1983 On the Monte-Carlo method for modeling particle dispersion in turbulence. In *Proceedings of Gas–Solid Flows*, Vol. 10, pp. 37–41. Fluids Engineering Div., ASME, New York.

CLEAVER, J. W. & YATES, B. 1975 A sub layer model for the deposition of particles from a turbulent flow. *Chem. Engng Sci.* **30**, 983–992.

CSANADY, G. T. 1963 Turbulent diffusion of heavy particles in the atmosphere. *J. atmos. Sci.* **20**, 201–208.

DAHNEKE, B. 1974 Diffusional deposition of particles. *J. Coll. Int. Sci., Notes* **48**, 520–522.

DAVIES, C. N. (Ed.) 1966 Deposition from moving aerosols. In *Aerosol Science*. Academic Press, London.

DAVIS, M. H. 1972 Collisions of small cloud droplets: gas kinetic effects. *J. atmos. Sci.* **29**, 911–920.

FERGUSON, J. R. 1986 The effects of fluid continuity on the turbulent dispersion of particles. Ph.D. Dissertation, Washington State Univ., Pullman.

FINNICUM, D. S. & HANRATTY, T. J. 1985 Turbulent normal velocity fluctuations close to a wall. *Phys. Fluids* **28**, 1654–1658.

FRIEDLANDER, S. K. & JOHNSTONE, H. F. 1957 Deposition of suspended particles from turbulent gas streams. *Ind. Engng Chem.* **49**, 1151–1156.

GOREN, S. L. & ERHART, D. L. 1989 Particle velocities normal to a wall for turbulent shear flow. *J. Fluid Mech.* In press.

HALL, D. 1988 Measurements of the mean force on a particle near a boundary in turbulent flow. *J. Fluid Mech.* **187**, 451–466.

HAPPEL, J. & BRENNER, H. 1965 *Low Reynolds Number Hydrodynamics*, pp. 322–331. Prentice-Hall, Englewood Cliffs, N.J.

HINZE, J. O. 1975 *Turbulence*, 2nd edn. McGraw-Hill, New York.

HUTCHINSON, P., HEWITT, G. F. & DUKLER, A. E. 1971 Deposition of liquid or solid dispersions from turbulent gas streams: a stochastic model. *Chem. Engng Sci.* **26**, 419–439.

KREPLIN, H.-P. & ECKELMANN, H. 1979 Behavior of the three fluctuating velocity components in the wall region of a turbulent channel flow. *Phys. Fluids* **22**, 1233–1239.

LAUFER, J. 1954 The structure of turbulence in fully developed pipe flow. NACA Report 1174, pp. 1–18.

LIU, B. Y. H. & AGARWAL, J. K. 1974 Experimental observation of aerosol deposition in turbulent flow. *Aerosol Sci.* **5**, 145–155.

LIU, B. Y.H. & ILORI, T. A. 1974 Aerosol deposition in turbulent flow. *Envir. Sci. Technol.* **8**, 351–356.

LUCHIK, T. S. & TIEDERMAN, W. G. 1987 Timescale and structure of ejections and bursts in turbulent channel flows. *J. Fluid Mech.* **174**, 529–552.

MAXEY, M. R. & RILEY, J. J. 1983 Equation of motion for a small rigid sphere in a nonuniform flow. *Phys. Fluids* **26**, 883–889.

PAPAVERGOS, P. G. & HEDLEY, A. B. 1984 Particle deposition behaviour from turbulent flows. *Chem. Engng Res. Des.* **62**, 275–295.

REEKS, M. W. 1977 On the dispersion of small particles suspended in an isotropic turbulent fluid. *J. Fluid Mech.* **83**, 529–546.

REEKS, M. W. 1982 COPDIRC—calculation of particle deposition in reactor coolants. CEGB Report TPRD/B/0016/N82.

REEKS, M. W. 1983 The transport of discrete particles in inhomogeneous turbulence. *J. Aerosol Sci.* **14**, 729–739.

REEKS, M. W. & SKYRME, G. 1976 The dependence of particle deposition velocity on particle inertia in turbulent pipe flow. *J. Aerosol Sci.* **7**, 485–495.

RIZK, M. A. & ELGHOBASHI, S. E. 1985 The motion of a spherical particle suspended in a turbulent flow near a plane wall. *Phys. Fluids* **28**, 806–817.

SAFFMAN, P. G. 1965 The lift on a small sphere in a slow shear flow. *J. Fluid Mech.* **22**, 385–400.

SAFFMAN, P. G. 1968 Corrigendum to "The lift on a small sphere in a slow shear flow". *J. Fluid Mech.* **31**, 624.

SATO, Y. & YAMAMOTO, K. 1987 Lagrangian measurement of fluid–particle motion in an isotropic turbulent field. *J. Fluid Mech.* **175**, 183–199.

SEHMEL, G. A. 1970 Particle deposition from turbulent air flow. *J. geophys. Res.* **75**, 1766–1781.

SHUEN, J-S., CHEN, L-D. & FAETH, G. M. 1983 Evaluation of a stochastic model of particle dispersion in a turbulent round jet. *AIChE Jl* **29**, 167–170.

WALLACE, J. M., ECKELMANN, H. & BRODKEY, R. S. 1972 The wall region in turbulent shear flow. *J. Fluid Mech.* **54**, 39–48.

WELLS, M. R. & STOCK, D. E. 1983 The effects of crossing trajectories on the dispersion of particles in a turbulent flow. *J. Fluid Mech.* **136**, 31–62.

YUU, S., YASUKOUCHI, N., KOROSAWA, Y. & JOTAKI, T. 1978 Particle turbulent diffusion in a dust laden round jet. *AIChE Jl* **24**, 509–519.